Photon TMDs from uPDFevolv

Hannes Jung[1], Sara Taheri Mondfared[1] and Thomas Wening[2]⋆

1 Deutsches Elektronen-Synchrotron, D-22607 Hamburg, Germany
2 II. Institute for Theoretical Physics, University of Hamburg, Germany

⋆ thomas.wening@desy.de

*Proceedings for the XXVIII International Workshop
on Deep-Inelastic Scattering and Related Subjects,
Stony Brook University, New York, USA, 12-16 April 2021*

Abstract

We present photon TMDs generated using the Parton Branching Method with QED evolution. We discuss the TMD's properties and compare it to the gluon TMD. Two sets of TMDs differing in their initial evolution scale and the choice of the renormalisation scale are defined and compared to each other.

1 Introduction

Parton distribution functions (PDFs) are an indispensable tool of quantum chromodynamics (QCD). They allow us to separate the non-perturbative physics in the infrared from the perturbatively calculable physics. PDFs help to describe the physics of the constituents of bound QCD states such as the proton. To each such parton we associate a (collinear) PDF $f_i(x, \mu^2, \mu_f^2)$. PDFs are functions which depend on the parton's longitudinal momentum fraction x, the renormalisation scale μ and the factorisation scale μ_f. In the past one has considered $i = q, g$ for the light quarks and the gluon. These days, one also considers heavy quarks, the photon [1,2] and the goal is to also include the heavy gauge bosons and the Higgs boson into the picture.

Transverse momentum dependent PDFs (TMDs) $A_i(x, \mu_f^2, \mu^2, \mathbf{k}_t)$ on the other hand are functions which additionally depend on the parton's transverse momentum $\mathbf{k}_t$ [3]. In the Parton Branching (PB) Method these are generated by relating the branching scale to the transverse momentum of the parton undergoing the branching cascade. Thereby, it accumulates transverse momentum with each branching and a TMD is obtained [4,5].

The PB Method has already been used successfully in the description of deep inelastic scattering (DIS) data at HERA and Drell-Yan (DY) data at the LHC [6,7]. Examples for processes in which TMDs are essential are the production of Z bosons at the LHC or the calculation of the proton's structure functions at small x [3]. The increasing accuracy of experimental data warrants an increase in precision for theoretical calculations and thus the use of TMDs is of the essence.

2 The PB Method in a Nutshell

The PDFs and TMDs are generated in via the PB Method. An initial parton at some initial factorisation scale $\mu_{f,0}^2$ undergoes a parton branching cascade up to the final factorisation scale μ_f^2. At each intermediate scale $t \in [\mu_{f,0}^2, \mu_f^2]$, the incoming mother parton splits into two daughter partons. One of these continues along in the cascade and may undergo further branchings. Its longitudinal momentum fraction z is determined by evaluating the kinematics at the branching point. The branching scale t is determined from the Sudakov form factor (SFF) $\Delta_i(z_m, \mu_f^2, \mu_{f,0}^2)$ of the mother parton i. The SFF is a measure of the probability for a resolvable branching *not* to occur between two branching scales t_0, t. It is given by

$$\Delta_i(t, t_0, z_m) = \exp\left(-\sum_j \int_{\ln t_0}^{\ln t} d\ln t' \int_0^{z_m} dz \, z P_{ji}^{(R)}\big(\alpha_s(\mu(t')), \alpha(\mu(t')), z\big)\right). \quad (1)$$
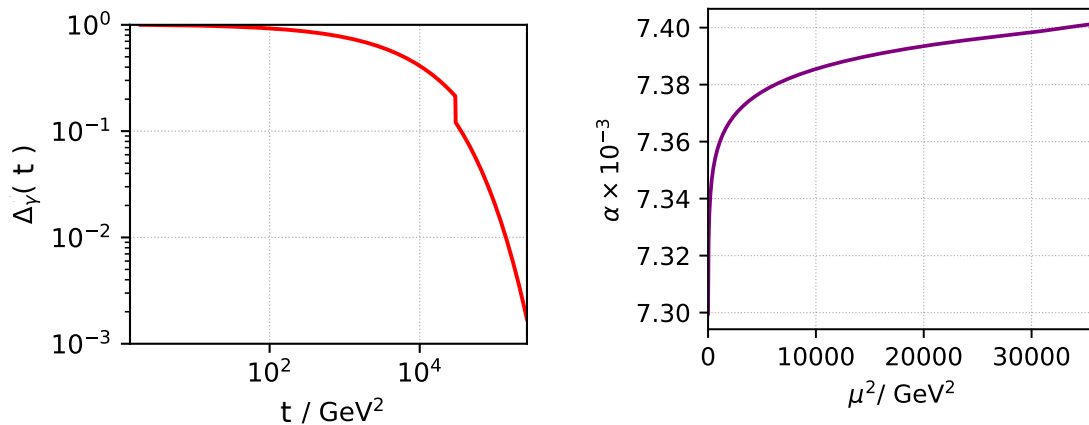
Figure 1: Left: Plot of the photon's SFF Δ_γ with the parameters $t_0 = 1.9$ GeV², $z_m = 1 - 10^{-6}$ and a running QED coupling with matching at the quark mass thresholds. Right: Plot of the running LO-QED coupling against the renormalisation scale μ^2.

Here, z_m with $1 - z_m \ll 1$ is the softness parameter, distinguishing unresolvable soft branchings ($z > z_m$) from the resolvable ones ($z < z_m$). Also, the functions $P_{ji}^{(R)}$ are the regular parts of the full splitting kernels P_{ji}. The LO-QED splitting kernels are given in [1]. Also, the strong and electromagnetic couplings α_s, α depend on the renormalisation scale $\mu(t')$ which itself may be chosen to depend on the branching scale t', over which one integrates.

It is important to note that instead of treating α_s, α as formally of the same order, one should adapt a phenomenological order counting [2] since $\alpha \sim \alpha_s^2$ over a wide range of scales μ^2. This means that using LO-QED splitting kernels requires the use of NLO-QCD splitting kernels. Moreover, lepton PDFs can be neglected because these would be of order $\mathcal{O}(\alpha^2)$.

The photon's SFF is depicted in Fig.1. At the scale $t \approx 3 \times 10^4$ GeV² one can see a discontinuity corresponding to the top quark mass. This is due to the fact that the photon can only branch into the quarks lighter than the top quark below this scale. As soon as the scale is above the top quark mass, the photon can also branch into a top quark. Since the SFF is a measure for the probability for the photon *not* to branch, it must descrease here because there are more branching channels available now. Similar disconuities lie at the bottom and charm quark masses and the explanation for those is analogous. These however, cannot be seen in this plot.

One is free to set both the branching scale t and the renormalisation scale μ^2 equal to some physical quantity of energy dimension two. Hence, we can define two sets according to the choice of the renormalisation scale μ^2. For Set 1 the renormalisation scale $\mu^2 = t$ is set equal to the branching scale t, for Set 2 $\mu^2 = \mathbf{k}_t^2$ the renormalisation scale is set equal to the square of the transverse momentum. Moreover, both sets are defined to differ in the initial factorisation scale: $\mu_{f,0}^2 = 1.9 \text{ GeV}^2$ for Set 1 and $\mu_{f,0}^2 = 1.4 \text{ GeV}^2$ for Set 2 [8].

One can relate the branching scale to the branching angle θ via the ordering condition $t = \mathbf{q}_t^2/(1-z)^2 = \mathbf{q}^2 \sin^2\theta$. This is called angular ordering. The parton in the branching cascade thus also accumulates transverse momentum $\mathbf{k}_t = \sum_i \mathbf{q}_t$ over the course of the evolution. The end result is a transverse momentum-dependent PDF $A_i(x, \mu_f^2, \mathbf{k}_t)$ which fulfils $\int \mathbf{k}_t^2 A_i(x, \mu_f^2, \mathbf{k}_t) = f_i(x, \mu_f^2)$ [4].

The PB method as described above is implemented for quarks and gluons in the code from [9]. A more detailed description can be found in [10]. A new version of the code also including the generation of PDFs and TMDs for the photon is under development.

3 The Photon TMD

We now want to present the results for the photon TMD. The soft parameter is $z_m = 1 - 10^{-6}$, the initial evolution scale is $\mu_{f,0}^2 = 1.9 \text{ GeV}^2$ in the following and angular ordering is used. Also, we have assumed $f_\gamma = 0$ at the starting scale, so no instrinsic photon density is assumed. In Fig.2, the photon TMD plotted against k_t is shown on the left and on the right one can see a comparison of the photon TMD against the gluon TMD.

In the plot on the left, one can see that the photon TMD increases for lower x-values. This is because at each branching, the momentum fraction of the daughter parton $z \in [x, z_m]$ is bounded below by the momentum fraction of the mother parton. This means that for higher x-values, the inteval $[x, z_m]$ is smaller. Additionally, the interval shrinks with each branching because x is the mother parton's momentum fraction and thus it increases with each branching. The angular ordering condition imposes a z-dependency in the generation of transverse momentum via $k_t^2 = (1-z)^2 t^2$ and so, the higher the z-value in a branching, the lower the k_t-contribution of that branching.

The TMD decays in the high-k_t region. This is because for high k_t-values to be generated, there must be many branchings with low z-values at the end of the cascade. If there have already been many branchings at lower scales, the consecutive branchings at higher scales do not contribute that much k_t since for high z we have $k_t = (1-z)t \ll t$ This also explains why the maximum k_t one can see in the plot increases with decreasing x-values.

One can see that the TMD is more or less constant in the low-k_t region up to $\sim 1.4 \text{ GeV}$. For low k_t-values to be generated during the cascade, there must be few branchings early on in the cascade for high z-values and even less branchings later in the cascade because those correspond to high transverse momenta due to the ordering condition. Now, assume a branching right at the beginning of the cascade at the initial evolution scale. Then we have $k_t = (1-z)\mu_{f,0} < \mu_{f,0}$ since $z \in [x, z_m]$. Note that the value of $1.4 \text{ GeV} \approx \sqrt{1.9 \text{ GeV}^2}$ corresponds to the initial evolution scale. For low x-values, the range of allowed z-values is large at the beginning of the cascade and hence the generated k_t will be lower than the initial evolution scale, depending on the z-value generated for the branching. That is why the TMD is more or less constant in the low-k_t region up to 1.4 GeV.

On the right-hand plot one can see that the gluon TMD is several orders higher than the photon TMD. This has several reasons. For one, the QED coupling $\alpha \sim \alpha_s^2$ is generally weaker than the QCD coupling. This means that a quark is more likely to split into a gluon than into a photon. Also, unlike the Abelian photon, the gluons are self-interacting and thus a gluon can
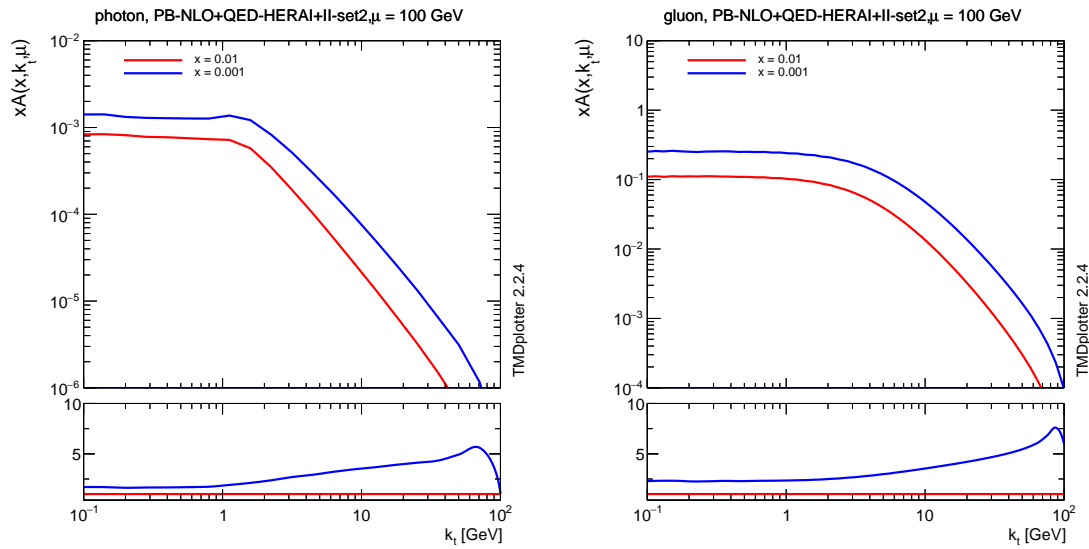
Figure 2: Left: Photon TMD plotted against k_t for the final evolution scale $\mu = 100$ GeV and two different x-values. Right: Gluon TMD plotted against k_t for the same final evolution scale. Note that the range of the y-axis is different in both plots.

split into another gluon. Some of the gluon density is thereby retained, whereas the photon can only split into a quark at a branching point. Last but not least, while there is an intrinsic gluon density, there is no intrinsic photon density. The entire photon TMD must be generated dynamically during the cascade.
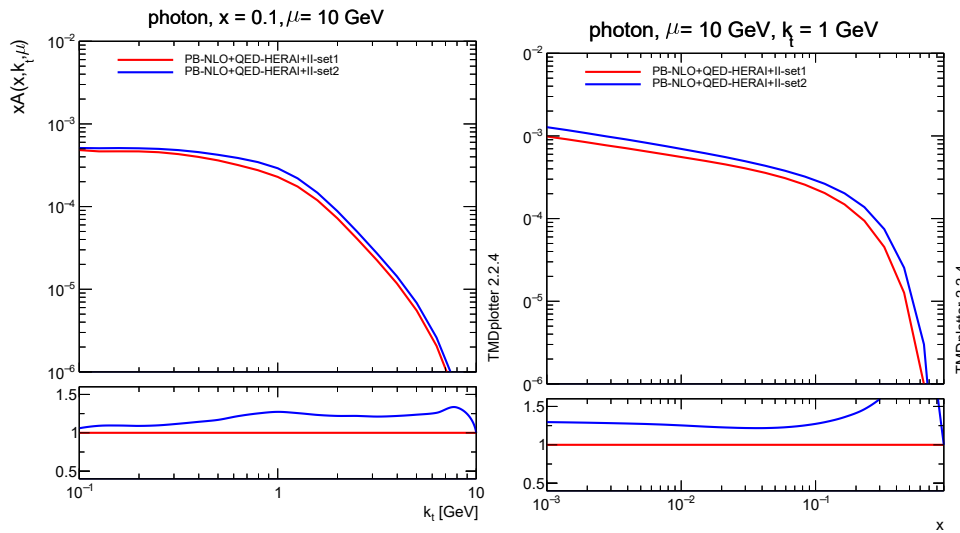
Figure 3: Comparison of photon TMDs for Set 1 and Set 2 plotted against k_t (left) and x (right).

In Fig.3, one can see a comparison of the photon TMDs for Set 1 and Set 2, once plotted against k_t (left) and against x (right). One can see that both TMDs look very similar in their shape, with the Set 2 TMD being higher than the Set 1 TMD. This is due to the difference in the initial evolution scale. With $\mu_{f,0}^2 = 1.9$ GeV^2 Set 2 has a higher initial evolution scale than Set 1 with $\mu_{f,0}^2 = 1.4$ GeV^2. This means that the former has a slightly longer evolution cascade

and more opportunities for branchings to occur where k_t can be generated. In Ref. [8] the transverse momentum spectrum of Z-bosons obtained from the two TMD sets (there without the photon TMDs) are compared to measurements from Ref. [11]. It is found that the Set 2 TMDs are in better agreement with the measurement data, especially in the low-k_t regime.

In Ref. [12] we also show the dilepton high mass distribution production compared to predictions at QCD+QED using Set2 PB-TMDs in the full phase space and the standard DY and PI transverse momentum spectra based on collinear and TMD PB-QED (Set2) at different high mass regions.

4 Conclusion

We have presented photon TMDs generated using the PB Method and we discussed their properties. We have seen that the photon TMDs have a plateau region for low k_t up to roughly the initial evolution scale which is due to the ordering condition imposed on them. We also saw that the photon TMDs decay for k_t-values above the initial evolution scale and that the lower the momentum fraction x, the higher the photon TMD. When comparing the photon to the gluon TMD, we have seen that the gluon TMD is several orders higher than the photon TMD due to the photon's lack of self-interaction, the lower electromagnetic coupling $\alpha \sim \alpha_s^2$ and the fact that there is no intrinsic photon density assumed. At last, we compared photon TMDs for the two different sets of renormalisation scale and initial evolution scale and saw that while both have the same overall shape, the Set 2 TMD was in general higher to to its lower initial evolution scale.

The photon TMDs from `uPDFevolv` can be used for precision QCD calculations and the next step should be to also introduce the electroweak sector to the Parton Branching formalism. To that end, Sudakov form factors for the heavy gauge bosons must be introduced, a means to distinguish polarised PDFs and electroweak splitting kernels.

Acknowledgements

This paper is based on the work presented in Ref. [12]. We thank F. Hautmann for various discussions and comments on the manuscript. STM thanks the Humboldt Foundation for the Georg Forster research fellowship.

References

[1] M. Roth and S. Weinzierl, *QED corrections to the evolution of parton distributions*, Phys. Lett. B **590**, 190 (2004), doi:10.1016/j.physletb.2004.04.009.

[2] A. V. Manohar, P. Nason, G. P. Salam and G. Zanderighi, *The photon content of the proton*, J. High Energy Phys. **12**, 046 (2017), doi:10.1007/JHEP12(2017)046.

[3] R. Angeles-Martinez et al., *Transverse Momentum Dependent (TMD) Parton Distribution Functions: Status and Prospects*, Acta Phys. Pol. B **46**, 2501 (2015), doi:10.5506/aphyspolb.46.2501.

[4] F. Hautmann, H. Jung, A. Lelek, V. Radescu and R. Žlebčík, *Collinear and TMD quark and gluon densities from parton branching solution of QCD evolution equations*, J. High Energy Phys. **01**, 070 (2018), doi:10.1007/jhep01(2018)070.

[5] F. Hautmann, H. Jung, A. Lelek, V. Radescu and R. Žlebčík, *Soft-gluon resolution scale in QCD evolution equations*, Phys. Lett. B **772**, 446 (2017), doi:10.1016/j.physletb.2017.07.005.

[6] A. Bermudez Martinez et al., *Production of Z bosons in the parton branching method*, Phys. Rev. D **100**, 074027 (2019), doi:10.1103/PhysRevD.100.074027.

[7] A. Bermudez Martinez et al., *The transverse momentum spectrum of low mass Drell–Yan production at next-to-leading order in the parton branching method*, Eur. Phys. J. C **80**, 598 (2020), doi:10.1140/epjc/s10052-020-8136-y.

[8] A. Bermudez Martinez, P. Connor, H. Jung, A. Lelek, R. Žlebčík, F. Hautmann and V. Radescu, *Collinear and TMD parton densities from fits to precision DIS measurements in the parton branching method*, Phys. Rev. D **99**, 074008 (2019), doi:10.1103/PhysRevD.99.074008.

[9] F. Hautmann, H. Jung and S. Taheri Monfared, *The CCFM uPDF evolution uPDFevolv Version 1.0.00*, Eur. Phys. J. C **74**, 3082 (2014), doi:10.1140/epjc/s10052-014-3082-1.

[10] A. Lelek, *Determination of TMD parton densities from HERA data and application to pp processes*, Ph.D. thesis, Hamburg U. (2018), doi:10.3204/PUBDB-2018-02949.

[11] G. Aad et al., *Measurement of the transverse momentum and ϕ^*_η distributions of drell–yan lepton pairs in proton–proton collisions at $\sqrt{s} = 8$ TeV with the atlas detector*, Eur. Phys. J. C **76**, 291 (2016), doi:10.1140/epjc/s10052-016-4070-4.

[12] H. Jung, S. Taheri Monfared and T. Wening, *Determination of collinear and TMD photon densities using the Parton Branching method*, Phys. Lett. B **817**, 136299 (2021), doi:10.1016/j.physletb.2021.136299.